THE JOURNAL OF BIOLOGICAL CHEMISTRY
Vol. 280, No. 15, Issue of April 15, pp. 14962–14973, 2005

Printed in U.S.A.

Crucial Role of Two Potential Cytosolic Regions of Nox2, ^{191}TSSTKTIRRS^{200} and ^{484}DESQANHFAVHHDEEKD^{500}, on NADPH Oxidase Activation*

Received for publication, January 7, 2005, and in revised form, January 27, 2005
Published, JBC Papers in Press, January 31, 2005, DOI 10.1074/jbc.M500226200

Xing Jun Li‡, Didier Grunwald§, Jacques Mathieu¶, Françoise Morel‡, and Marie-José Stasia‡‖

From the ‡Groupe de Recherche et d'Etude du Processus Inflammatoire EA 2938 Université Joseph Fourier, Laboratoire Enzymologie, Centre Hospitalier Universitaire, 38043 Grenoble cedex 9, the §Département Réponse et Dynamique Cellulaire/Commissariat à l'Energie Atomique, 17 rue des Martyrs, 38054 Grenoble cedex 9, and the ¶Département de Radiobiologie, Centre de Recherches du Service de Santé des Armées, 38702 La Tronche cedex, France

Assembly of cytosolic factors p67^{phox} and p47^{phox} with cytochrome b_{558} is one of the crucial keys for NADPH oxidase activation. Certain sequences of Nox2 appear to be involved in cytosolic factor interaction. The role of the D-loop ^{191}TSSTKTIRRS^{200} and the C-terminal ^{484}DESQANHFAVHHDEEKD^{500} of Nox2 on oxidase activity and assembly was investigated. Charged amino acids were mutated to neutral or reverse charge by directed mutagenesis to generate 21 mutants. Recombinant wild-type or mutant Nox2 were expressed in the X-CGD PLB-985 cell model. K195A/E, R198E, R199E, and RR198199QQ/AA mutations in the D-loop of Nox2 totally abolished oxidase activity. However, these D-loop mutants demonstrated normal p47^{phox} translocation and iodonitrotetrazolium (INT) reductase activity, suggesting that charged amino acids of this region are essential for electron transfer from FAD to oxygen. Replacement of Nox2 D-loop with its homolog of Nox1, Nox3, or Nox4 was fully functional. In addition, fMLP (formylmethionylleucylphenylalanine)-activated R199Q-Nox2 and D-loop$_{Nox4}$-Nox2 mutants exhibited four to eight times the NADPH oxidase activity of control cells, suggesting that these mutations lead to a more efficient oxidase activation process. In contrast, the D484T and D500A/R/G mutants of the α-helical loop of Nox2 exhibited no NADPH oxidase and INT reductase activities associated with a defective p47^{phox} membrane translocation. This suggests that the α-helical loop of the C-terminal of Nox2 is probably involved in the correct assembly of the NADPH oxidase complex occurring during activation, permitting cytosolic factor translocation and electron transfer from NADPH to FAD.

Baldridge and Gerard (1, 2) discovered the respiratory burst in which dramatic oxygen consumption occurred in neutrophils during bacteria phagocytosis. Subsequent research showed that the NADPH oxidase complex of phagocytic cells is responsible for the innate host defense by producing superoxide anions (O_2^-) and reactive oxygen species to kill invading bacterials and fungi (3–6). The importance of this system is demonstrated by chronic granulomatous disease (CGD),[1] characterized by severe and recurrent life-threatening infections, resulting in defective NADPH oxidase activity (7–10). However, recent evidence indicates that the killing activity of neutrophils is mediated through activation of proteases by K^+ flux, and the large-conductance Ca^{2+}-activated K^+ channel is essential for innate immunity (2, 11). NADPH oxidase is a multicomponent complex, composed of a heterodimeric transmembrane protein known as flavocytochrome b_{558}, cytosolic proteins p47^{phox}, p67^{phox}, and p40^{phox}, and two small GTPase, Rac2 and Rap1A. Cytochrome b_{558}, the redox core of the respiratory burst oxidase, consists of a large glycoprotein gp91^{phox} or Nox2 and a small protein p22^{phox} (12). Nox2 is the catalytic center that transfers the electrons from intracellular NADPH to extracellular O_2. It contains two nonidentical hemes and consensus-binding sequences for FAD and NADPH (13–16). NADPH oxidase becomes activated and generates O_2^- after cytosolic factor assembly with cytochrome b_{558}. In the resting state, p67^{phox} connects p40^{phox} and p47^{phox} by its PB1 and C-terminal SH3 domains with the PC domain of p40^{phox} and the proline-rich region of p47^{phox}, respectively (17). Upon activation, a series of protein-protein interactions occurs. The phosphorylation of p47^{phox} causes a conformational change of the protein, which leads to binding the membrane phosphoinositides and the proline-rich region of p22^{phox} with its PX domains and SH3, respectively (18–22). p22^{phox} serves as a docking site for p47^{phox} and an accessory for p67^{phox}. p67^{phox} was shown to be involved in both assembly and activation of the oxidase complex, whereas p47^{phox} proceeded as a positive effector and increased the affinity of p67^{phox} with cytochrome b_{558} (23, 24). Current evidence suggests that there is a direct interaction between p67^{phox} and cytochrome b_{558}, promoted by Rac1-p67^{phox} binding (25–26). However, the precise sequence of the p67^{phox} and cytochrome b_{558} interaction has not been fully elucidated. In PMA-stimulated phagocytes from X-CGD patients, no translocation of p47^{phox}, p67^{phox}, and p40^{phox} to the membranes occurs, indicating that gp91^{phox} is absolutely required for the binding of cytosolic components to cytochrome b_{558} (27).

Sequence alignment of Nox2 with members of the ferredoxin-reductase family demonstrates the presence of six transmembrane α-helices in the N-terminal hydrophobic region, four cytosolic regions, the ^{1}MGNWVAVNEGL^{11}sequence, the B-

* This work was supported by grants from the Université Joseph Fourier, Faculté de Médecine; the Région Rhône-Alpes, programme Emergence and programme conjoint de recherche Tempra/Mira 2001; the Ministère de l'Education et de la Recherche; and the Direction de la Recherche Régionale Clinique, Laboratoire Merck-Sharp and Dohme-Chibret. The costs of publication of this article were defrayed in part by the payment of page charges. This article must therefore be hereby marked "*advertisement*" in accordance with 18 U.S.C. Section 1734 solely to indicate this fact.

‖ To whom correspondence should be addressed. Tel.: 33-4-7676-5483; Fax: 33-4-7676-5608; E-mail: MJStasia@chu-grenoble.fr.

[1] The abbreviations used are: CGD, chronic granulomatous disease; PMA, phorbol 12-myristate 13-acetate; fMLP, formylmethionylleucylphenylalanine; DMF, dimethylformamide; GTPγS, 5′-3-*O*-(thio)triphosphate; BCS, broken cell system; WT, wild type; FACS, fluorescence-activated cell sorting; INT, iodonitrotetrazolium.

loop ^{70}PVCRNLLSFLRGSSACCSTRIRRQLDRNLTFHK^{102}, the D-loop ^{191}TSSTKTIRRS^{200}, and a C-terminal region containing binding sites for FAD, NADPH, and cytosolic components of NADPH oxidase (12). A peptide inhibitory study, random-sequence peptide phage analysis, and the mutagenesis approach suggested that complementary binding sites of gp91^{phox} encompassing residues ^{451}FEWFADLL^{458} and ^{559}RGVHFIF^{565} presumably interact with cytosolic factors upon stimulation (19, 21, 28–35). Furthermore, mutations in Nox2 found in X$^+$CGD cases (C369R, G408E, E568K, and H303N/P304R) have been reported to abolish the oxidase assembly (36–40). In addition, Taylor *et al.* (28) had predicted a three-dimensional structure of Nox2 using ferredoxin-NADP$^+$ reductase as template and proposed that an α-helical loop ^{491}FAVHHDEEKDVITG^{504} covers the cleft in which NADPH binds. During oxidase activation, access of NADPH into the binding site could potentially be regulated by interaction of this loop with cytosolic oxidase factors. However, there were conflicting results for the role of this potential α-helical loop. Leusen and co-workers found that cytosolic factors p47^{phox} and p67^{phox} did not translocate to the plasma membrane of phagocytes from an X$^+$CGD case because of the D500G missense mutation located in this sequence of gp91^{phox}. In addition, a peptide mimicking 491–504 residues of Nox2 inhibited the translocation of p47^{phox} and p67^{phox} to the membrane (30). In contrast, in another X$^+$CGD case consisting of a Δ488–497 gp91^{phox} deletion in the α-helical loop, translocation of p47^{phox} and p67^{phox} to the plasma membrane occurred normally (40). Recently Dinauer and co-workers have studied the role of a second cytosolic region of Nox2, the B loop, on oxidase activity (35). They found that two Arg at positions 91 and 92 were essential for NADPH oxidase activity and assembly. However, the role of the second intracytosolic polybasic loop of Nox2, the D-loop ^{191}TSSTKTIRRS^{200}, has never been elucidated.

Recently, large homologs of gp91^{phox}, called Nox and Duox, have been identified. They are present in various tissues of nonphagocytic cells and can generate low amounts of O_2^-, suggested to be involved in cell signaling, host defense, hypoxia response, and also as proton transport (41). The family contains seven members in humans. Nox1, Nox3, and Nox4 resemble Nox2 in that they consist of six α-helix transmembrane regions in the N-terminal, with two intracytosolic loops (B and D-loops) and a cytosolic C-terminal tail containing the putative binding sites for FAD and NADPH (42). A recent study indicates that p51 and p41 (homolog of p67^{phox} and p47^{phox}, respectively) regulate Nox1 to generate O_2^- (43–46). This suggests that Nox proteins need some cytosolic components to be activated or regulated. Meanwhile, the molecular mechanisms of the regulation of Nox2 homologs has not been fully elucidated.

The aim of this work was to investigate the role of two regions of Nox2, the intracytosolic D-loop ^{191}TSSTKTIRRS^{200} and the C-terminal α-helical loop ^{484}DESQANHFAVHHDEEKD^{500}, on oxidase activity and assembly by means of the mutagenesis approach in the X-CGD PLB-985 cell model (37). Results suggest that these two regions are critical for NADPH oxidase activity, especially the charged amino acids Arg^{195}, Arg^{198}, Arg^{199}, Asp^{484}, and Asp^{500}. The D-loop of Nox2 is probably involved in electron transfer from FAD to oxygen independently of cytosolic factor translocation, whereas the C-terminal α-helical loop is crucial for the assembly of oxidase and electron transfer from NADPH to FAD. Chimeric Nox2 proteins containing the D-loop of Nox1/3/4 support NADPH oxidase activity, suggesting that this region should play a similar role on Nox analog activation. Finally, two "super-mutants" of the D-loop of Nox2, with a significant increase in oxidase activity, were obtained, suggesting that the R199Q and D-loop$_{Nox4}$ mutations optimize the NADPH oxidase activation process.

EXPERIMENTAL PROCEDURES

Materials—Phorbol 12-myristate 13-acetate (PMA), dimethylformamide (DMF), diisopropylfluorophosphate, and horseradish peroxidase, cytochrome *c* (horse heart, type VI), and latex beads were obtained from Sigma. *Taq*DNA polymerase, ATP, GTPγS, and NADPH were from Roche Applied Science. Endofree Plasmid Maxi Kit was purchased from Qiagen. The Sephaglas kit and molecular weight markers for SDS-PAGE were from Amersham Biosciences. Nitrocellulose sheets for Western blotting were purchased from Bio-Rad. G418 was purchased from Invitrogen. Monoclonal antibodies 449 and 48 were kindly provided by Dr. D. Roos (Sanquin Research at CLB, Amsterdam, the Netherlands). Polyclonal antibody anti-p47^{phox} (rabbit antiserum) was purchased from Upstate Biotechnology, Inc. (New York, NY). Monoclonal antibody specific for gp91^{phox}, 7D5 was kindly provided by Dr. M. Nakamura (Nagasaki University, Nagasaki, Japan). Fetal bovine serum and RPMI 1640 were from Invitrogen.

Site-directed Mutagenesis and Expression of Recombinant gp91^{phox} in X-CGD PLB-985 Cell Line—Mutations were introduced into the wild-type (WT) Nox2 cDNA in pBluescript II KS(+) vector using the QuikChange site-directed mutagenesis kit (Stratagene) according to the manufacturer's instructions. The sequence of WT and the mutated gp91^{phox} cDNA were verified by dideoxynucleotide sequencing (Genome Express, Grenoble, France). The WT or mutant Nox2 cDNA were subcloned into the mammalian expression vector pEF-PGKneo as previously described (37). The pEF-PGKneo constructs were electroporated into X-CGD PLB-985 cells in which the gp91^{phox} gene was disrupted by gene targeting, resulting in the absence of Nox2 expression and NADPH oxidase activity as previously described (37, 38). Clones were selected by limiting dilution in 1.5 mg/ml G418.

Cell Culture and Granulocyte Differentiation—WT, X-CGD, and transfected PLB-985 cells expressing WT or the mutant were maintained in RPMI 1640 supplemented with 10% (v/v) fetal bovine serum, 100 units/ml penicillin, 100 μg/ml streptomycin, 2 mM L-glutamine at 37 °C in a 5% CO_2 atmosphere. After selection, 0.5 mg/ml G418 was added to maintain the selection pressure. PLB-985 cells (5×10^5 cells/ml) were exposed to 0.5% DMF for 5–7 days, providing granulocytic differentiation as described previously (38).

Analysis of Nox2 Protein Expression—PLB-985 cells (5×10^5) were incubated with 10 μg/ml of mAb 7D5 directed against Nox2 or control monoclonal IgG1 (Immunotech, Marseille, France). Then the cells were incubated with phycoerythrin-labeled goat-F(ab′)$_2$ fragment anti-mouse-Ig (Beckman Coulter, Marseille, France). Finally, flow cytometry analysis (FACS) was performed (FACSCalibur, BD Biosciences) (48). Sorting of 7D5-positive PLB-985 cells was done on a FACSVantage Diva (BD Biosciences) instrument at a sheath pressure of 12 p.s.i. with a 70-μm nozzle. Cells were collected into phosphate-buffered saline supplemented with 0.5% bovine serum albumin and routinely contained >97% of 7D5-positive cells. Viability after sorting was >95%. After centrifugation of the cell suspension, the cell pellet was resuspended in culture medium. The expression of recombinant Nox2 was also examined by Western blot using monoclonal antibody 48 developed with the ECL detection system (Amersham Pharmacia Biotech) as described previously (49). The WT or mutant Nox2 expression was further detected indirectly by cytochrome b_{558} differential spectral analysis. A molecular extinction coefficient of Σ426 nm = 106 mM^{-1} × cm^{-1} for the Soret band was used for calculations (50). All experiments were done in triplicate.

Cytosol and Membrane Fraction Preparation from Transfected PLB-985 Cell Lines—10^8 PLB-985 cells were treated with 3 mM diisopropylfluorophosphate for 15 min on ice and resuspended in 1 ml of phosphate-buffered saline containing 1 mM phenylmethylsulfonyl fluoride, 2 μM leupeptin, 2 μM pepstatin, and 10 μM 1-chloro-3-tosylamido-7-amino-2-heptanone. Cells were disrupted by sonication, and the homogenate was centrifuged at 1,000 × *g* for 15 min at 4 °C. The supernatant was withdrawn and centrifuged at 152,000 × *g* for 1 h at 4 °C. This high speed supernatant was referred to as the cytosol, and the pellet consisting of crude membranes was resuspended in the same buffer, as described before (51).

Measurement of NADPH Oxidase Activity in Intact Cells—H_2O_2 production was measured as described previously (38). For each well in a 96-well plate, 5×10^5 granulocytic differentiated PLB-985 cells in phosphate-buffered saline with 0.9 mM Ca^{2+} and 0.5 mM Mg^{2+} was mixed with 20 mM glucose, 20 μM luminol, and 10 units/ml horseradish peroxidase. We added 80 ng/ml PMA to initiate the reaction. Luminescence was recorded every 30 s for a total of 90 min at 37 °C using a Luminoscan® luminometer (Labsystems, Helsinki, Finland). In some experiments, PMA was replaced by 4×10^{-7} M fMLP.

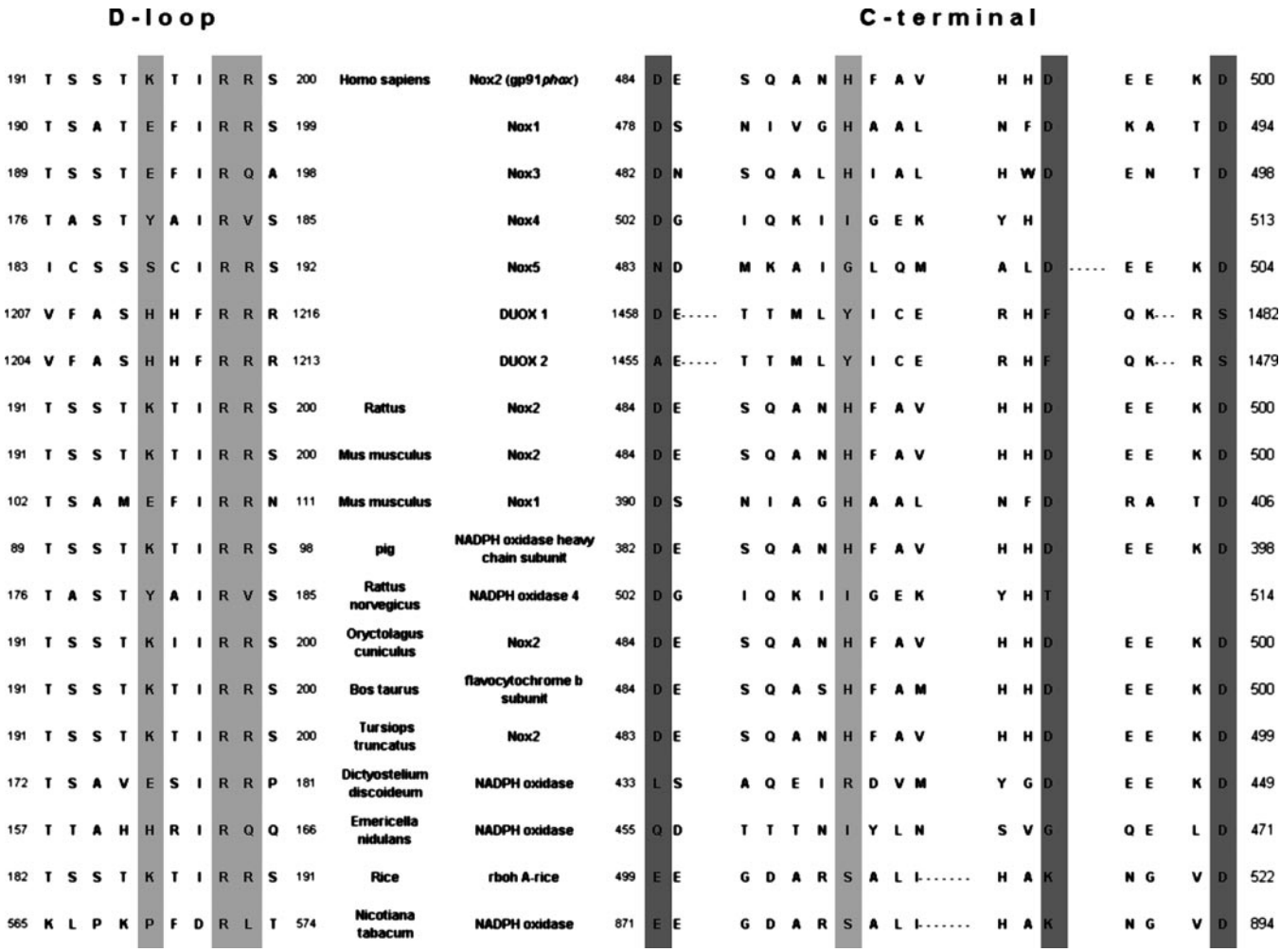

FIG. 1. **Amino acid sequence alignment of the D-loop (^{191}TSSTKTIRRS^{200}) and the C-terminal (^{484}DESQANHFAVHHDEEKD^{500}) of Nox2 in the ferredoxin NADP$^+$ family.** Positive charged amino acid residues are shown in the *light shaded column*, Asp residues are shown in the *dark shaded column*.

Detection of NADPH Oxidase Activity in a Broken Cell System—NADPH oxidase activity *in vitro* was measured in a homologous BCS using previously described protocols (52). Briefly, plasma membranes obtained from transgenic PLB-985 cells and cytosol of control human neutrophils were added to a reaction mixture containing 20 mM glucose, 20 μM GTPγS, 5 mM $MgCl_2$, and arachidonic acid in a final volume of 100 μl. After incubation for 10 min at 25 °C, the oxidase activation was initiated in the presence of 100 μM cytochrome *c* and 150 μM NADPH. The specificity of the O_2^- production was checked by adding 50 μg/ml superoxide dismutase to stop the kinetic reduction.

Iodonitrotetrazolium Reductase Activity—Diaphorase activity was measured under the same BCS assay conditions, except that the 100 μM cytochrome *c* was replaced by 50 μM INT (53).

Analysis of in Vivo p47^{phox} Translocation—In vivo p47^{phox} translocation was detected by confocal microscopy analysis according to (38) with little modified. The 5×10^5 differentiated PLB-985 cells deposited on coverslips were activated with PMA-treated latex beads (3 μm in diameter) at 37 °C for 15 min. The cells were fixed in 4% paraformaldehyde for 10 min and permeabilized with 0.1% Triton X-100. After extensive washing, cells were incubated for 1 h at room temperature with the diluted polyclonal anti-p47^{phox} (Upstate Biotechnology Inc.). After washing, cells were incubated in 5% bovine serum albumin/phosphate-buffered saline buffer containing a 2-μg/ml Alexa Fluor® 488 F(ab′)$_2$ fragment of goat anti-rabbit IgG(H+L) (Molecular Probes, Eugene, OR) for 1 h. Finally, PLB-985 cells were stained with 3 μM TO-PRO 3 iodide for 10 min to visualize the nuclei. Cells were examined with a confocal laser scanning microscope and analyzed with Leica confocal software (Heidelberg, Germany). In some experiments, a 10 μg/ml mAb 7D5 and a 4-μg/ml Alexa Fluor® 546 F(ab′)$_2$ fragment of goat anti-mouse IgG(H+L) (Molecular Probes) were added to the system as primary and secondary antibodies, respectively, to detect Nox2.

Analysis of Translocation of p47^{phox} in Vitro—In vitro p47^{phox} translocation to the plasma membrane was measured using a classic protocol (37). Briefly, membranes purified from PLB-985 cells (100 μg) were preincubated with human neutrophil cytosol (1,000 μg) for 2 min at 30 °C and activated with (+) or without 100 μM SDS and 20 μM GTPγS for 15 min at 30 °C. Membranes were collected between the 45 and 20% (w/v) sucrose layers after centrifugation (30,000 rpm $\times$ 1 h in an SW41 rotor (Beckman) at 18 °C) and analyzed using immunoblotting with anti-peptide polyclonal antibody directed against p47^{phox} (24).

Protein Determination—Protein content was estimated using the Bradford assay (54) or the Pierce® method (55).

RESULTS

To further understand the role of the D-loop (^{191}TSSTK-TIRRS^{200}) and the C-terminal (^{484}DESQANHFAVHH-DEEKD^{500}) in Nox2 upon oxidase activation, homologous sequence analysis in the ferredoxin-NADP$^+$ reductase family was done (Fig. 1). The D-loop is a polybasic region, containing Lys^{195}, Arg^{198}, and Arg^{199}, which are conserved in the ferredoxin-NADP$^+$ reductase family. In the C-terminal, the charged amino acids encompassing residues 484–500 are also highly conserved in this family, especially Asp^{484}, His^{490}, Asp ^{496}, and Asp^{500}. We postulated that charged amino acids within these two domains might be important for the active conformation of Nox2 and/or for further binding with cytosolic factors. Hence charged amino acid residues were replaced with neutral or reverse-charged residues by site-directed mutagenesis to alter the local electrostatic charge within these

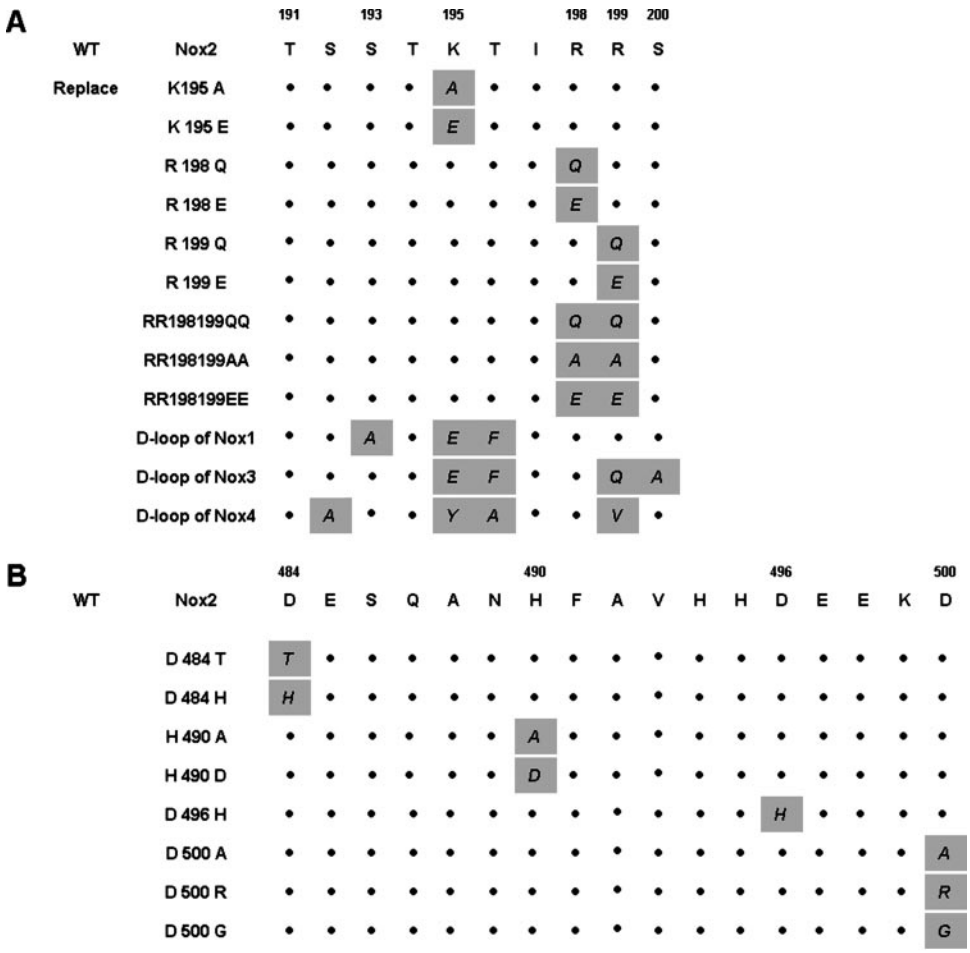

FIG. 2. **Mutagenesis of the two potential cytosolic loops ^{191}TSSTKTIRRS^{200} and ^{484}DESQANHFAVHHDEEKD^{500} of Nox2.** *A*, the D-loop Thr^{191}–Ser^{200}; *B*, the α-helical loop in the C-terminal (Asp^{484}–Asp^{500}). The wild-type amino acid sequences of Nox2 are shown in the *top line*, and the mutant sequences are shown in *shaded boxes*. The *dots* indicate the amino acid residues that are identical to the wild-type sequence. Three to four amino acids are changed simultaneously to replace the D-loop of Nox2 with the same region of its homolog. An X^+ CGD mutation (D500G) is reconstituted (30).

two regions (Fig. 2). To further elucidate the function of the D-loop in the Nox family, the D-loop of Nox2 was replaced with the same region of their homologs Nox1, Nox3, and Nox4. Twelve mutants of the D-loop (Fig. 2A) and eight of the α-helical loop in the C-terminal of Nox2 (Fig. 2*B*) were generated by directed mutagenesis and stably transfected in X-CGD PLB-985 cells, which lack endogenous Nox2 expression because of gene targeting (56). We also produced two mutants known to disturb cytosolic factor translocation to the plasma membrane, the D500G mutant, which had reproduced a human X^+CGD case (30), and the RR9192EE mutant of the B loop of Nox2 previously studied by Biberstine-Kindade *et al.* (35). These two mutants served as controls to validate NADPH oxidase activity and assembly experiments.

The WT and mutated Nox2 cDNA subcloned into the pEF-PGKneo vector were verified by sequence analysis and purified before transfection in X-CGD PLB-985 cells, as described under "Experimental Procedures." Nox2 expression was studied by FACS using the monoclonal antibody 7D5, and IgG1 were used as negative control to test the specificity of Nox2 binding (38). For some mutants, FACS was also used to sort a highly Nox2-expressing population. This was done for K195A, RR198199QQ (data not shown), and K195E mutant cells (Fig. 3*A*). We detected 12–20 different clones for each mutant and to minimize clone-to-clone variation in NADPH oxidase activity, three to four independent clones of each highly expressing Nox2 mutant were used for subsequent analysis (data not shown). As expected, Nox2 was not detected in X-CGD PLB-985 cells or in empty vector transfected PLB-985 cells. Expression of WT or mutant Nox2 was also assessed by semiquantitative immunoblotting of soluble extracts from differentiated WT and transfected X-CGD PLB-985 cells using the monoclonal antibody 48 (38). Similar Nox2 expression was seen in all differentiated PLB-985 cells (Fig. 3*B*). Identical differential spectrum characteristics of flavocytochrome b_{558} were observed in all mutants compared with WT Nox2-transfected PLB cells or WT PLB-985 cells (data not shown). The amount of cytochrome b_{558} was equivalent in all the transfected X-CGD PLB-985 cells, confirming results previously obtained by FACS and Western blot analysis (Table I). This demonstrated correct heme incorporation in recombinant Nox2. No differential spectra were detected in X-CGD PLB-985 cells or empty vector-transfected cells. In conclusion, high, stable, and similar amounts of recombinant WT or mutant Nox2 proteins were expressed in transfected X-CGD PLB-985 cells. This was crucial for comparing the impact of each mutation on NADPH oxidase functions in such cells.

We next measured H_2O_2 production in transfected X-CGD PLB-985 cells stimulated by 80 ng/ml PMA using luminol-amplified CL. The RR9192EE Nox2 transfected PLB-985 cells exhibited no oxidase activity, whereas its cytochrome b_{558} expression was comparable to the WT Nox2-transfected PLB-985 cells (Table I). This was consistent with previously published results (35) and allowed us to validate our methodology.

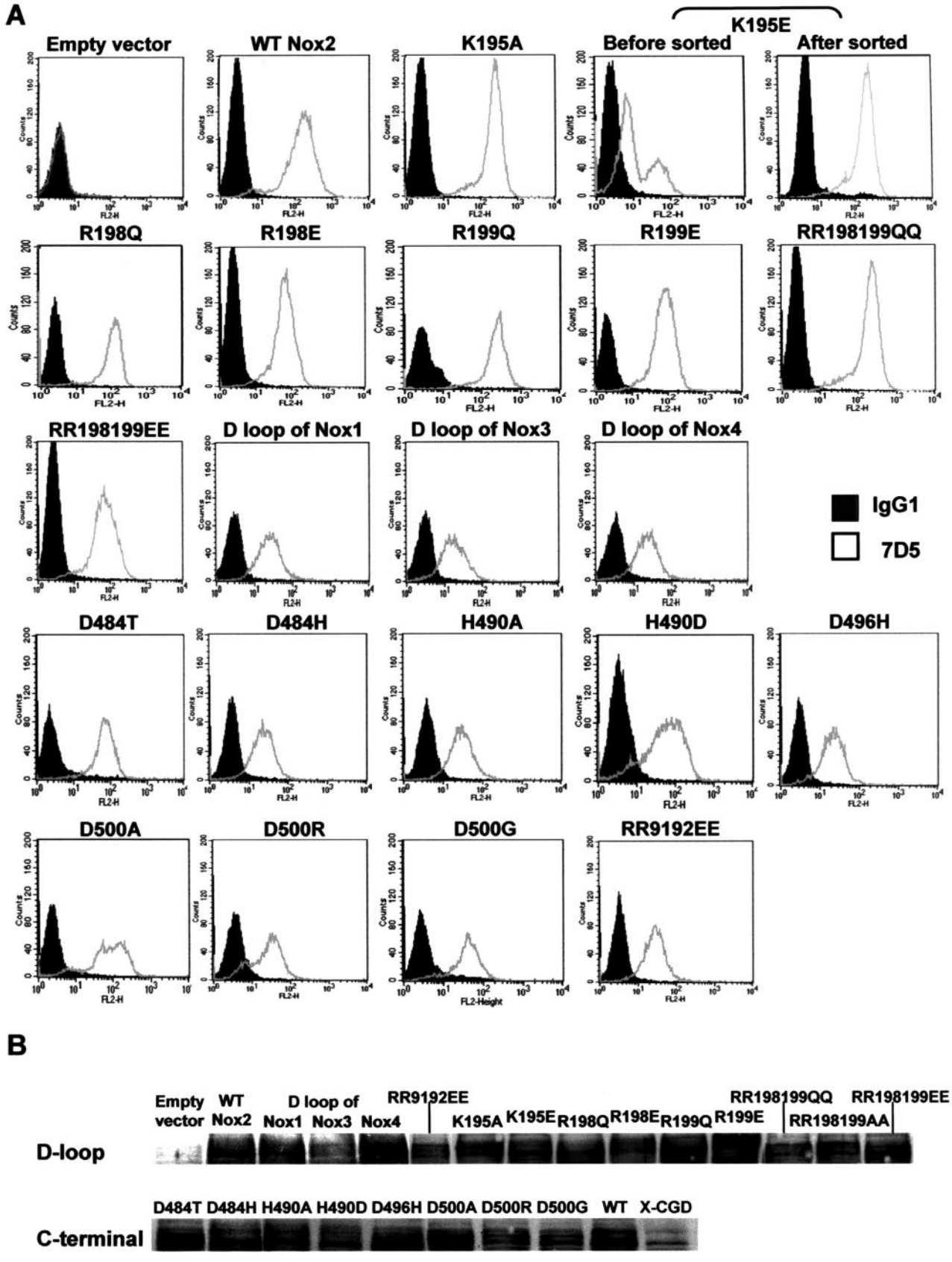

FIG. 3. **Expression of WT and mutated Nox2 in transfected X-CGD PLB-985 cells.** *A*, 5×10^5 transfected X-CGD PLB-985 cells were incubated with the gp91^{phox} monoclonal antibody 7D5, combined with a phycoerythrin-conjugated goat-anti-IgG (*H+L*) as described under "Experimental Procedures." Mouse IgG1 isotype was used as an irrelevant monoclonal antibody. *B*, immunodetection of gp91^{phox} subunits of cytochrome b_{558} (*Nox2*) was performed with 50 μg of 1% Triton X-100 soluble extracts from WT or transfected X-CGD PLB-985 cells, subjected to SDS-PAGE (10% acrylamide gel), blotted onto a nitrocellulose sheet, and revealed with mAb 48 monoclonal antibodies. Results are from one experiment representative of three.

TABLE I

Cytochrome b_{558} amount and NADPH activity in WT and transfected X-CGD PLB-985 cells

The cytochrome b_{558} concentration was quantified using Soret band absorption of 1% Triton X-100-soluble extracts from WT, X-CGD, and mutant transfected PLB-985 cells, considering that cytochrome b_{558} contains two hemes. H_2O_2 production was measured by luminol-amplified CL for 90 min in differentiated WT and transfected X-CGD PLB-985 cells after PMA activation. RLU represents the sum of relative luminescence units measured in 90 min. NADPH oxidase activity was reconstituted in a broken cell system (BCS) with purified plasma membranes of the indicated cells (30 μg) in the presence of neutrophil cytosol (300 μg) and activated with GTPγS and arachidonic acid as described under "Experimental Procedures." Values represent the mean ± S.D. of triplicate determinations.

	Transgenic PLB-985 cells	Cytochrome b_{558}	Chemiluminescence		Cell-free-system	
			H_2O_2 production	% of control	O_2^- production	% of control
		pmol/mg	*RLU*	*%*	*nmol/min/mg protein*	*%*
	WT PLB-985 cells	26.27 ± 2.96	397.75 ± 5.07	100	93.37 ± 17.74	100
	WT Nox2 cells	24.36 ± 2.31	453.02 ± 4.19	114	96.00 ± 23.21	103
	X-CGD PLB-985 cells	0	0.68 ± 0.03	0	0.00 ± 3.79	0
	Empty vector	0	0.66 ± 0.07	0	0.93 ± 5.04	1
B-loop	RR9192EE	21.79 ± 0.46	0.27 ± 0.02	0	3.02 ± 4.79	3
D-loop	K195A	16.69 ± 0.22	0.73 ± 0.01	0	21.94 ± 8.88	23
	K195E	22.04 ± 1.00	0.16 ± 0.05	0	6.24 ± 5.04	7
	R198Q	22.20 ± 2.62	255.23 ± 1.47	64	72.54 ± 16.72	71
	R198E	21.35 ± 1.81	0.17 ± 0.01	0	7.95 ± 6.95	9
	R199Q	22.75 ± 2.45	562.75 ± 17.85	141	94.77 ± 12.63	101
	R199E	24.18 ± 1.60	0.16 ± 0.02	0	9.29 ± 3.71	10
	RR198199QQ	27.86 ± 0.45	0.16 ± 0.02	0	19.67 ± 2.72	21
	RR198199EE	23.42 ± 1.55	240.69 ± 4.76	61	48.96 ± 15.58	52
	D-loop of NOX 1	23.67 ± 2.10	521.75 ± 3.94	131	111.03 ± 5.32	119
	D-loop of NOX 3	15.98 ± 0.79	497.73 ± 5.13	125	118.00 ± 14.14	126
	D-loop of NOX 4	20.28 ± 0.72	646.93 ± 11.11	163	113.99 ± 9.16	122
C-terminal	D484T	16.92 ± 5.73	0.37 ± 0.04	0	12.41 ± 1.65	13
	D484H	22.86 ± 0.18	314.28 ± 17.77	79	71.98 ± 6.31	77
	H490A	22.41 ± 0.68	451.03 ± 2.10	113	90.08 ± 8.75	94
	H490D	21.02 ± 0.46	40.49 ± 1.00	10	31.76 ± 2.91	34
	D496H	24.47 ± 3.45	405.29 ± 16.16	102	72.50 ± 16.7	78
	D500A	15.02 ± 1.36	0.25 ± 0.02	0	11.33 ± 3.51	12
	D500R	25.42 ± 0.97	0.54 ± 0.01	0	8.46 ± 7.79	9
	D500G	19.78 ± 0.53	0.12 ± 0.04	0	4.05 ± 2.93	4

NADPH oxidase activity was completely abolished in cells expressing K195A/E, R198E, R199E, and RR198199QQ mutations of the D-loop of Nox2. The RR198199AA mutation had the same inhibitory effect on oxidase activity as the RR198199QQ mutation (data not shown). However, cells expressing R198Q-Nox2 and RR198199EE-Nox2 mutants exhibited almost 60% of NADPH oxidase activity measured in WT PLB-985 cells. Surprisingly, transfected R199Q and D-loop$_{Nox1/3/4}$ Nox2 mutant PLB-985 cells stimulated with PMA had an increase of 1.3- to 1.6-fold in H_2O_2 production compared with the WT PLB-985 cells (Table I). In the C-terminal tail of Nox2, changing Asp^{484} to a neutral amino acid (D484T) inhibited the NADPH oxidase activity, whereas replacing it with a positive charge (D484H) had little effect (79% of control). In addition, the D496H mutation had no effect on oxidase activity. However, cells expressing H490A-Nox2 exhibited normal oxidase activity, whereas the H490D mutation destroyed most of the NADPH oxidase activity (10% of control) (Table I). In conclusion, the effect of D484 and H490 charge changes had different effects on oxidase activity depending on the type of amino acid replacement. Meanwhile, the disappearance of the negative charge supported by Asp^{500} in the D500A, D500R, and D500G mutations had a definitive inhibitory effect on NADPH oxidase activity (Table I). It should be noted that the D500G Nox2-transfected cells mimicked the phenotype of a previously described X^+ CGD case (30).

To improve our knowledge of H_2O_2 production in DMF-differentiated transfected X-CGD PLB-985 cells, PMA and fMLP stimulation were compared (Fig. 4*A*). All the experiments were done in triplicate and reproduced twice. Inhibitory effects of some mutations on oxidase activity, observed previously in PMA-stimulated PLB-985 cells, were also obtained in fMLP-activated mutant cells. The increasing effect on NADPH oxidase activity of the R199Q mutation and the replacement of the Nox2 D-loop with the same from Nox1/3/4, was more evident using fMLP stimulation. Indeed in the R199Q and the D-loop$_{Nox4}$ mutant cells, H_2O_2 production was 7.9 and 4.6 times higher than in the WT PLB-985 cells, respectively (Fig. 4*A*). The kinetics of H_2O_2 production was not the same when WT or WT Nox2-transfected PLB-985 cells were activated by PMA or fMLP (Fig. 4*B*). The maximum of H_2O_2 production (V_{max}) was obtained in 10–13 min (T_{max}) for PMA activation, whereas for fMLP, the T_{max} was reached in roughly 4 min (Table II). Interestingly, the V_{max} for the D-loop$_{Nox4}$-Nox2 super-mutant cells activated with PMA was obtained in 4–5 min *versus* 10–13 min in WT PLB-985 cells. However, when these cells were stimulated with fMLP, the kinetics of H_2O_2 production remained unchanged, whereas the V_{max} was higher than in the WT PLB-985 cells (Fig. 4*B* and Table II). The same kinetic changes in H_2O_2 production were also observed in the R199Q mutant cells (data not shown).

We also examined the *in vitro* NADPH oxidase activity of transfected X-CGD PLB-985 cells using a broken cell system (BCS). To compare only the effect of mutations on Nox2 of the plasma membranes purified from transfected PLB-985 cells, cytosol from human neutrophils was used as the source of NADPH oxidase cytosolic components. The *in vitro* oxidase activity was totally restored in X-CGD PLB-985 transfected with WT Nox2 cDNA compared with WT PLB-985 cells (Table I). For almost all the studied mutations, the results obtained in BCS were correlated with those obtained in intact cells, although residual oxidase activity (~20% of the original WT PLB-985 cells) was observed in some mutants that had no oxidase activity *in vivo*. In addition, the highly increased NADPH oxidase activity measured in intact R199Q and in the D-loop$_{Nox4}$-Nox2 mutant cells activated with fMLP was not reconstituted *in vitro*.

As demonstrated above, mutations within these two cytosolic regions of Nox2 (K195A/E, R198E, R199E, RR198199QQ, D484T, and D500A/R/G) completely abolished the NADPH ox-

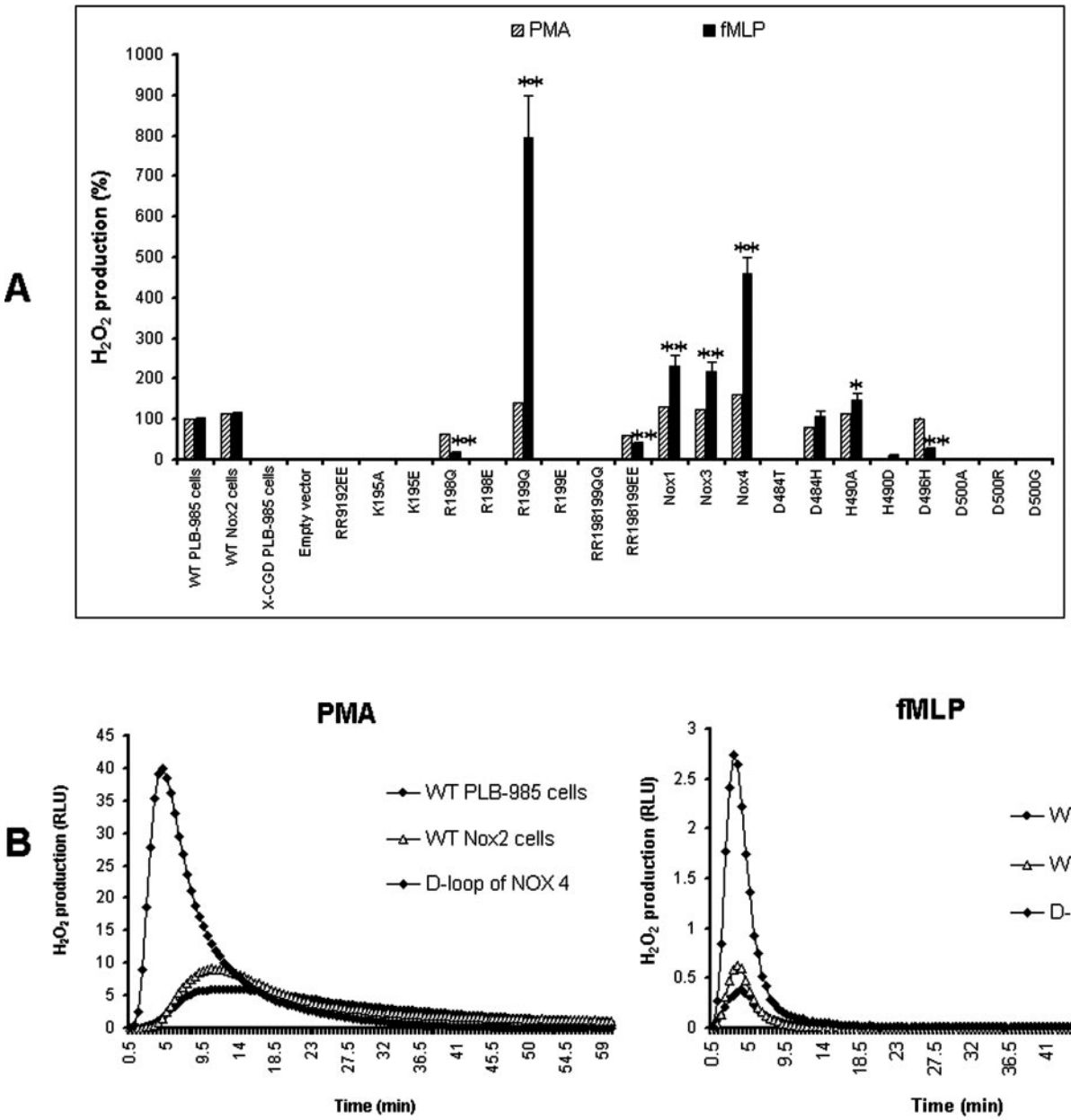

FIG. 4. **H_2O_2 production in WT and in transfected X-CGD PLB-985 cells after PMA and fMLP activation.** *A*, total H_2O_2 production was measured by luminol-amplified CL from 5×10^5 intact WT or transfected X-CGD PLB-985 cells differentiated with 0.5% DMF for 6 days and stimulated with 80 ng/ml PMA or 4×10^{-7} M fMLP. Results are expressed in a percentage by dividing the total RLU value obtained for each type of cells by the value of WT PLB-985 cells. Values in this figure represent the mean ± S.D. of triplicate determinations obtained the same day. The same experiment was done twice on 2 different days. *, $p < 0.05$; **, $p < 0.01$. *B*, kinetics of H_2O_2 production in 5×10^5 intact WT, or WT Nox2, or D-loop$_{Nox4}$-Nox2 transfected X-CGD PLB-985 cells stimulated either by 80 ng/ml PMA or 4×10^{-7} M fMLP.

TABLE II

Kinetics of H_2O_2 production in WT and in X-CGD transfected PLB-985 cells

H_2O_2 production in intact 5×10^5 differentiated WT or transfected X-CGD PLB-985 cells was measured using the chemiluminescence method after activation by 80 ng/ml PMA or 4×10^{-7} M fMLP for 90 min. Values represent the mean ± S.D. of triplicate determinations. V_{max} indicates the maximum of H_2O_2 production obtained. T_{max} indicates the time to V_{max}, which was measured as the elapsed time from the start of the assay until the maximum H_2O_2 production was obtained.

		WT PLB-985 cells	WT Nox2 cells	D-loop of NOX 4
PMA	Total H_2O_2 production (RLU)	397.75 ± 5.07	453.02 ± 4.19	646.93 ± 11.11
	T_{max} (min)	13.17 ± 1.44	10.83 ± 0.58	4.67 ± 0.29
	V_{max} (RLU)	5.94 ± 0.18	9.06 ± 0.17	38.9 ± 0.97
fMLP	Total H_2O_2 production (RLU)	4.65 ± 0.26	5.32 ± 0.15	22.79 ± 1.98
	T_{max} (min)	4.00 ± 0.00	3.50 ± 0.00	2.83 ± 0.29
	V_{max} (RLU)	0.40 ± 0.03	0.66 ± 0.04	3.07 ± 0.57

idase activity. To investigate the effect of these mutations on oxidase complex assembly, we used the confocal microscopy method, which allowed us to follow $p47^{phox}$ translocation to the plasma membrane in intact cells after stimulation, and in some experiments Nox2 localization was visualized by 7D5 recognition. To fully express $p47^{phox}$, $p67^{phox}$, $p40^{phox}$, and $gp91^{phox}$

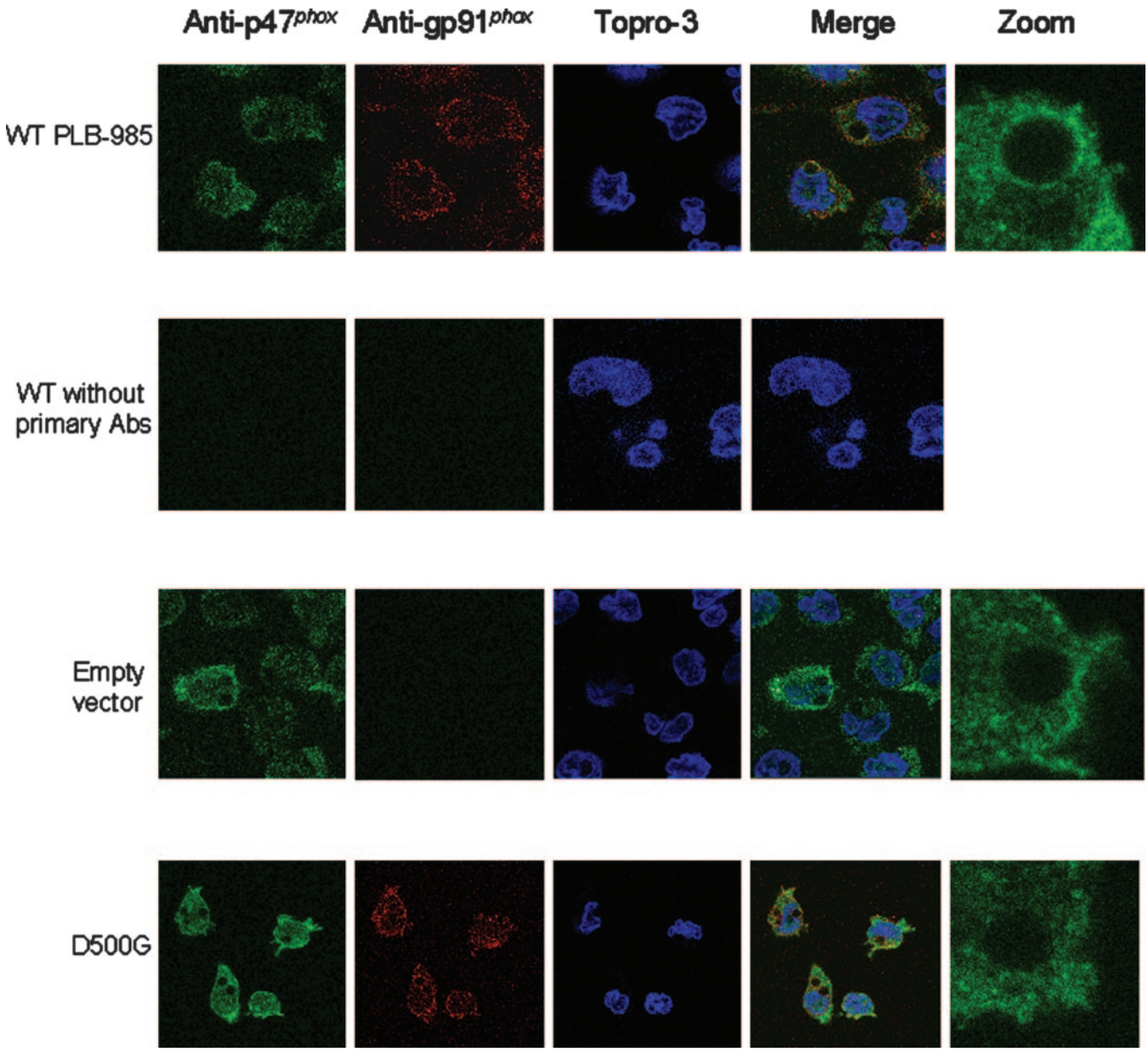

FIG. 5. **Localization of p47^{phox} and Nox2 during activation of WT PLB-985 cells, empty vector or X$^+$CGD PLB-985 cells.** A total of 5 × 10^5 WT or transfected X-CGD PLB-985 cells was stimulated with PMA-treated latex beads for 15 min on day 6 after 0.5% DMF differentiation. Nox2 and p47^{phox} translocation was followed by confocal microscopy analysis as described under "Experimental Procedures." Polyclonal anti-p47^{phox} Ab and monoclonal 7D5 were used as primary antibodies, Alexa Fluor 488 and Alexa Fluor 546 F(ab′)$_2$ fragments of goat anti-mouse IgG(H+L) were used as second antibodies. Negative control was provided by incubating differentiated WT PLB-985 cells with phosphate-buffered saline, 5% albumin instead of primary antibodies. The D500G-Nox2 transfected X-CGD PLB-985 cells mimicked an X$^+$ CGD case previously described (30).

(57), PLB-985 WT or mutated cells were differentiated by 0.5% DMF for 6 days before PMA-treated latex-bead stimulation, as described under "Experimental Procedures." For each translocation experiment, NADPH oxidase activity was measured the same day. The deformation of the TO-PRO 3 iodine-labeled nuclei allowed us to ascertain that the latex beads were indeed in the cell. As seen in Fig. 5, the phagocytosis of latex beads occurred in WT PLB985 cells as in empty-vector transfected X-CGD PLB-985 cells and in X$^+$CGD PLB-985 cells (D500G mutant) independently of oxidase activity. As expected, p47^{phox} protein was present in cytosol from all the tested PLB-985 cells. No fluorescence was observed in WT PLB-985 cells when primary antibodies were omitted. The *Red* and *Green* fluorescence colors representing Nox2 and p47^{phox}, respectively, surrounded the phagosome membranes around the latex beads only in intact WT PLB-985 cells (Fig. 5). A *yellow merged image* indicated the co-localization of p47^{phox} and Nox2 in phagosome membranes. However, the D500G-Nox2 mutation disrupted p47^{phox} membrane translocation. Nox2 was localized in phagosome and plasma membranes, whereas p47^{phox} was uniformly distributed in the cytosol, confirming previously published results (30) and confirming this method. In K195A/E, R198E, R199E, and RR198199QQ mutations, as the RR198199AA mutation (data not shown) in the D-loop of Nox2, which totally inhibited NADPH oxidase activity, a strong green fluorescence was seen surrounding phagocytosed latex particles (Fig. 6*A*), suggesting that the p47^{phox} protein translocated normally to the phagosome membranes. Other mutations generated in the D-loop of Nox2 had no influence on NADPH oxidase assembly (data not shown). In contrast, in some mutants of the α-helical loop of the C-terminal of Nox2 (D484T, D500A, and D500R) with no oxidase activity, the p47^{phox} membrane translocation

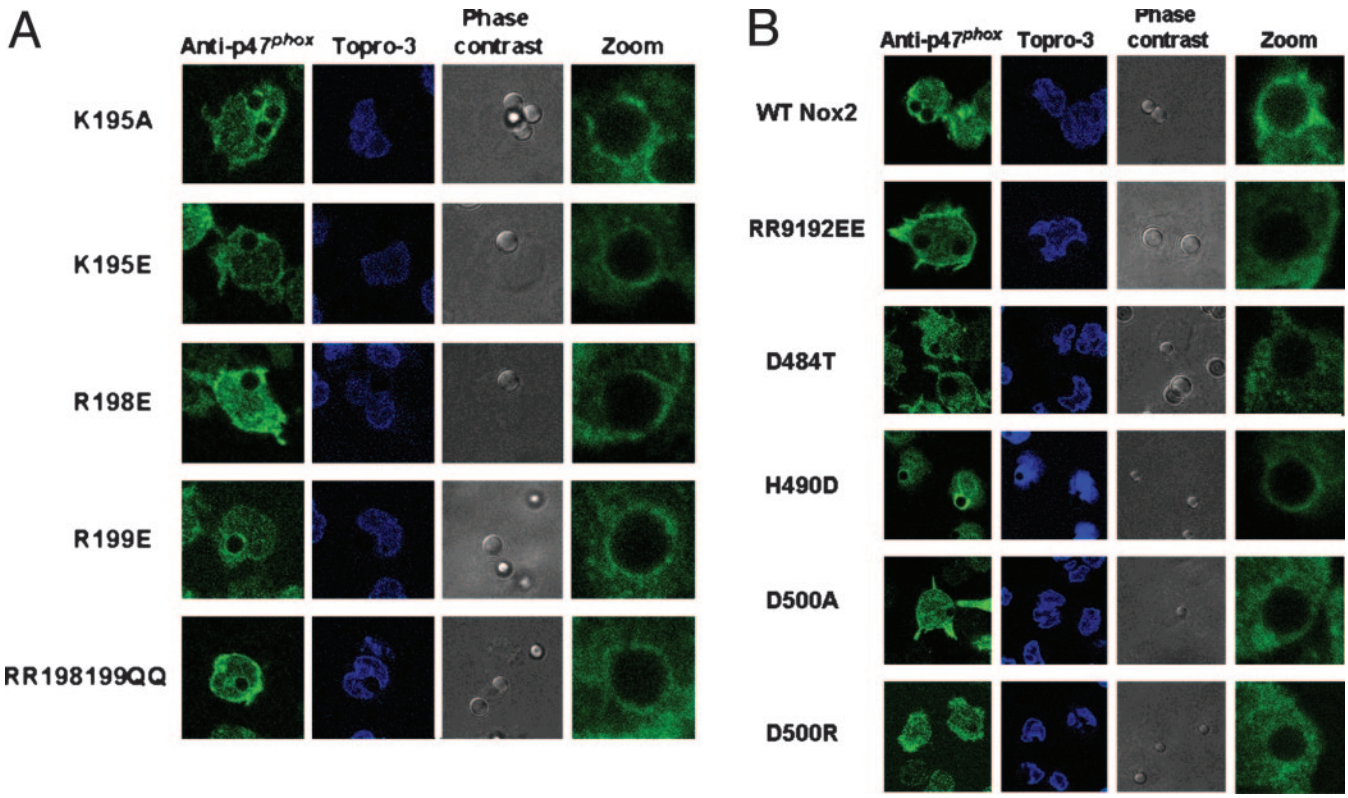

FIG. 6. **Study of NADPH oxidase assembly in transfected X-CGD PLB-985 cells stimulated by latex beads.** p47^{phox} translocation was followed by confocal microscopy analysis in transfected X-CGD PLB-985cells stimulated by PMA-treated latex beads as described under "Experimental Procedures." *A*, mutant PLB-985 cells of the potential D-loop of Nox2 exhibiting no oxidase activity. *B*, mutant PLB-985 cells of the potential α-helical loop of the C-terminal of Nox2 in which the NADPH oxidase activity is abolished. Negative control of p47^{phox} translocation was done by using RR9192EE-Nox2 mutant PLB-985 cells (35), whereas WT Nox2-transfected X-CGD PLB-985 cells were used as a positive control of p47^{phox} translocation.

was totally disrupted, as in the RR9192EE mutant of the B loop of Nox2, previously studied by Biberstine-Kankade *et al.* (35). However, in the H490D-Nox2-transfected PLB-985 cells that had ~10% activity of original WT PLB-985 cells, a normal p47^{phox} translocation occurred as in WT Nox2-transfected PLB-985 cells (Fig. 6*B*). Similar results were obtained from *in vitro* translocation experiments using purified plasma membranes from transfected X-CGD PLB-985 cells after SDS and GTPγS stimulation (Fig. 7). The *in vitro* p47^{phox} translocation was normal for K195A/E, R198E, R199E, and RR198199QQ/AA-Nox2-transfected PLB-985 cells similar to WT PLB-985 cells (data not shown) or WT Nox2 PLB-985 cells. In contrast, the p47^{phox} membrane translocation was defective in the D484T and in the D500A/R/G-Nox2 mutant cells. As expected, no p47^{phox} translocation occurred in the X-CGD PLB-985 cells (data not shown), in the empty vector transfected X-CGD PLB cells, or in the cells expressing the RR9192EE Nox2 mutant (Fig. 7*A*) (35).

Finally, diaphorase activity was measured in purified plasma membranes from WT or transfected mutant X-CGD PLB-985 cells (Fig. 8). Cytochrome b_{558} from WT Nox2-transfected cells supported INT reductase activity to the same extent as was assessed in original WT PLB-985 cells, whereas in the empty vector-transfected X-CGD PLB-985 cells, this activity was null. While the K195A/E, R198E, R199E, and RR198199QQ mutants of the D-loop of Nox2 had a totally abolished oxidase activity, they exhibited 80% INT activity of the WT PLB-985 cells (Fig. 8). However, D484T and D500G mutations in the α-helical loop of the C-terminal of Nox2 led to the inhibition of NADPH oxidase and INT reductase activities. This was also observed in D500A/R mutant cells (data not shown).

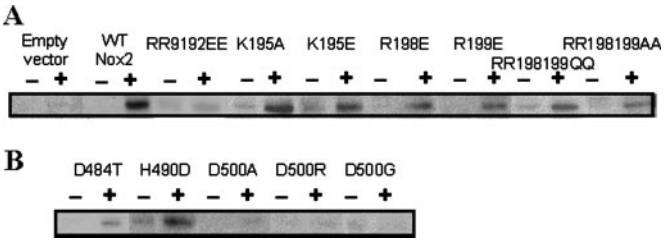

FIG. 7. **In vitro p47^{phox} translocation to the plasma membrane of transfected PLB-985 cells.** NADPH oxidase was activated *in vitro* in presence (+) or in absence (−) of SDS and GTPγ S, using purified membrane from mutant PLB-985 cells of the D-loop (Thr^{191}–Ser^{200}) (*A*) or the C-terminal (Asp^{484}–Asp^{500}) (*B*) of Nox2 as described under "Experimental Procedures." p47^{phox} was detected in the plasma membranes by Western blot after discontinuous sucrose gradient purification.

DISCUSSION

The NADPH oxidase of phagocytic cells is an enzymatic complex assembled from membranous cytochrome b_{558} and cytosolic components, p67^{phox}, p47^{phox}, p40^{phox}, and Rac2, upon cellular activation by microorganisms or/and inflammatory stimuli. The objective of this study was to examine the role of two cytosolic domains of Nox2 encompassing residues 191–200 (D-loop) and residues 484–500 (C-terminal) of Nox2 in NADPH oxidase function and assembly (30, 34). The D-loop has never been studied, whereas the C-terminal region of Nox2 was previously identified, by a predicted three-dimensional structure of Nox2, as an α-helical loop constituting a potential binding site for cytosolic factors (35). A point mutation D500G in this region in an X^{+}CGD case led to inhibition of cytosolic factor translocation to the plasma membrane of patient's neutrophils, confirming the previous hypothesis. However, in a second case

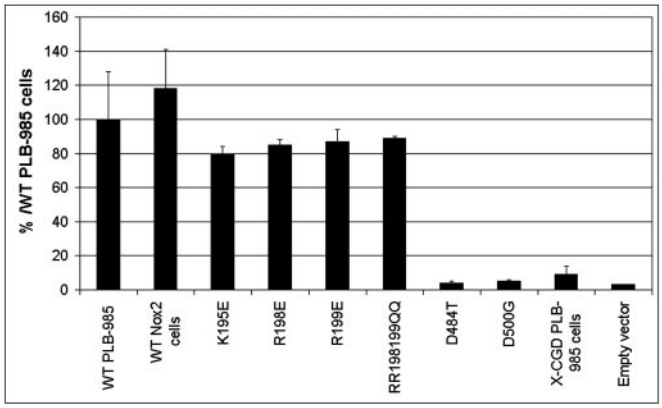

FIG. 8. **Diaphorase activity in a cell-free system assay using cellular membranes isolated from transfected X-CGD PLB-985 cells.** Diaphorase activity was determined in the same conditions as described above, except that cytochrome *c* was replaced with INT. The data represent mean ± S.D. of three separate experiments.

of X^+CGD caused by a Δ488–497 gp91^{phox} deletion in the α-helical loop, p47^{phox} and p67 ^{phox} translocation was normal, whereas electron transfer from NADPH to FAD was disturbed (40). In this study, we used site-directed mutagenesis to probe the role of specifically charged amino acid residues within the D-loop and the C-terminal α-helical loop of Nox2, hypothesizing that electrostatic interactions between charged residues of Nox2 and cytosolic factors may be important for assembly of the active NADPH oxidase complex. To study the functional effect of these mutations we chose the granulocytic cell line PLB-985 as the cellular model, so as to be close to physiological events occurring in phagocytic cells.

We found that the D-loop and the C-terminal α-helical loop of Nox2 played a crucial role in oxidase activity. We demonstrated that the positive charge of Lys^{195} was essential, because reversal or cancellation of it inhibited the NADPH oxidase activity (Table I). In addition, reversal of the electrostatic charge of Arg^{198} or Arg^{199} induced more inhibitory effects on NADPH oxidase activity than its cancellation. In contrast, when these two arginines were mutated simultaneously by opposite residues (RR198199EE), more than half of the oxidase activity could be measured in intact cells and in an *in vitro* reconstituted oxidase system (BCS). However, their replacement by two neutral residues (RR198199QQ) or two alanines (RR198199AA, data not shown) inhibited the oxidase activity (Table I). These data suggest that the total electrostatic charge at positions 198 and 199 is essential for NADPH oxidase activity. Interestingly, replacing Arg^{199} with a glutamine as in Nox3, increased oxidase activity *in vivo*, pointing out that this amino acid could play a specific role in oxidase activation process. Lys^{195} of the D-loop of Nox2 is highly conserved in Nox2 proteins from different species, including animals and plants, but it is highly variant in the human Nox family (Fig. 1), suggesting it has a special function in Nox2. In contrast, Arg^{198} is absolutely conserved in all the members of the Nox family, whereas Arg^{199} is replaced by neutral amino acids in Nox3 and Nox4. Within the past 4 years, Nox2 homologs have been identified in various tissues that have similar features to Nox2 and can generate modest superoxide (41, 42). However, although their structural arrangement is similar to Nox2, molecular mechanisms involved in reactive oxygen species production and activity regulation is unclear. We found that the three mutants in which the D-loop of Nox2 was replaced by the same region of Nox1, Nox3, or Nox4 exhibited high NADPH oxidase activity (Table I), although the electrostatic charge in this region was changed (Fig. 2*B*). This showed that the D-loop of Nox analogs is functional for the Nox2 activation process, suggesting that this loop should have a similar function in the Nox family. Negative-charged amino acids Asp^{484}, Asp^{496}, and Asp^{500} localized in the α-helical loop of the C-terminal of Nox2 are also essential for NADPH oxidase activity. Cancellation of the negative charge of Asp^{484} by replacement with a neutral amino acid (Thr) abolishes the NADPH oxidase activity in intact transfected PLB-985 cells as in an *in vitro* reconstituted oxidase system (BCS). However, a basic residue change (His) at this position can restore most of the oxidase activity, suggesting that a charged amino acid (Asp or His) at position 484 is essential for NADPH oxidase activity. In contrast, reversal of the charge at position 490 (H490D) significantly affects superoxide production. The most important acidic amino acid in this C-terminal region is probably Asp^{500}. Indeed all the mutations (D500A/R/G) of Nox2 inhibited *in vivo* and *in vitro* oxidase activity (Table I). In addition, the existence of two X^+CGD cases attributable to mutations in this region highlight the importance of this C-terminal domain on oxidase functioning (30, 58). Two other Asp^{500} mutations (D500Y/N) were reported in a CYBB data base (bioinf.uta.fi/CYBBbase/CYBBbase-browser.html). Negative-charged amino acids, Asp^{484}, Asp^{496}, and Asp^{500}, in the α-helical loop of the C-terminal of Nox2 are highly conserved in the ferredoxin-$NADP^+$ reductase family, however the basic amino acid His^{490} is present in Nox1, Nox3, and in Nox2 proteins from different species (Fig. 1). We should emphasize that any introduced mutation had no effect on the Nox2 maturation and stability because in all the transfected PLB-985 cells mutant Nox2 expression was normal (Fig. 3).

Interestingly, our data show the difference in the NADPH oxidase activity measured in some mutant-transfected X-CGD PLB-985 cells depending on the different type of stimulus employed to activate the enzyme. The slight H_2O_2 overproduction observed in PMA-stimulated mutant PLB-985 cells expressing the R199Q and the D-loop$_{Nox4}$ Nox2 proteins (super-mutant cells) was particularly exacerbated when these cells were activated with fMLP (Fig. 4*A*). In addition, the activation kinetics of the NADPH oxidase in WT PLB-985 cells, WT Nox2 PLB-985 cells, and D-loop$_{Nox4}$-Nox2 mutant PLB-985 cells activated with fMLP was more rapid and transient than with PMA. However, the H_2O_2 production kinetics was not changed in all the fMLP-activated PLB-985 cells, whereas this production was more rapid in PMA-activated D-loop$_{Nox4}$-Nox2 mutant PLB-985 cells (Fig. 4*B* and Table II) and in R199Q mutant cells only (data not shown). It is known that the kinetics of oxidase activation is not the same when human neutrophils are stimulated by fMLP or by PMA, because the signaling cascades triggered by these two agents are different. The high production of H_2O_2 in the D-loop$_{Nox4}$ and the R199Q-Nox2 mutant PLB-985 cells activated by PMA or fMLP may be due to a conformational change of the mutated Nox2 in the assembly of the NADPH oxidase complex, promoting a more efficient electron transfer to reduce molecular oxygen. If we admit that the H_2O_2 production is the result of an equilibrium between an active and inactive state of the NADPH oxidase, we can speculate that the mutations lead to a conformational change in favor of the active state of the enzyme. The difference in the activation level of the oxidase complex in the super-mutant PLB-985 cells stimulated by either PMA or fMLP can be due to different phosphorylation states of the cytosolic factors induced by these stimuli (8), leading to a more or less efficient interaction between them and the mutated D-loop$_{Nox4}$ and R199Q-Nox2 proteins. This hypothesis is supported by the fact that the oxidase activity of these two super-mutants in the reconstituted system (BCS), where no phosphorylation occurs, is not higher than in the WT-PLB-985 cells (Table I). The same difference between oxidase activity measured in intact PLB-985

cells and the *in vitro* reconstituted oxidase activity was previously observed in the study of the R91T/R92A mutant of the B loop of Nox2. Indeed the different kinetics of O_2^- production in this mutant activated by opsonized zymosan and PMA could be explained by different phosphorylation states of $p47^{phox}$ (35). In conclusion, the phosphorylation state of the cytosolic factors occurring *in vivo* may be essential to generate a "super-efficient" oxidase complex, including the D-$loop_{Nox4}$ or the R199Q-Nox2 proteins. However, it does not mean that the D-loop of Nox2 is *directly* involved in cytosolic factor binding. We should note that only mutations in the D-loop produce super-mutant PLB-985 cells, pointing out a crucial role of this region on NADPH oxidase activation. In addition, only two X-CGD mutations in the D-loop of Nox2 were described. The first case was a deletion in a codon corresponding to Arg^{199} leading to the creation of a premature stop codon at position 213 (59). The second one was a X-CGD case originated from a S193F missense mutation, suggesting that this region is possibly involved in the conformational stability of cytochrome b_{558} (60).

To elucidate the reason why the NADPH oxidase activity was abolished in some mutant PLB-985 cells, assembly of the oxidase complex was studied. Translocation of $p47^{phox}$ was followed by confocal microscopy in intact differentiated PLB-985 cells during latex-bead activation (Figs. 5 and 6). Experiments were conducted in all the mutant PLB-985 cells, and the data obtained were confirmed by the *in vitro* translocation experiment (Fig. 7). We previously described the same type of approach using opsonized zymosan particles (38). Using latex beads opsonized with human IgG or serum AB, we found a significant background in nonphagocytosed particles due to unspecific recognition by the fluorescent secondary antibody. We decided to use the latex particle method coated with PMA, as previously described to purify phagosome membranes (61, 62). Although K195A, K195E, R198E, R199E, and RR198199-QQ/AA mutations in the D-loop of Nox2 led to total oxidase inhibition, the $p47^{phox}$ translocation process was normal, suggesting that basic amino acids of this region do not participate in the direct binding of oxidase cytosolic factors (Fig. 6*A*). This suggests that translocation of $p47^{phox}$ and oxidase activation are two dissociated processes. However, mutant PLB-985 cells of the C-terminal of Nox2 (D484T, D500A/R/G mutations) with no oxidase activity had a $p47^{phox}$ translocation defect (Fig. 6*B*). This result is consistent with the hypothesis that when the oxidase is in a resting state, the potential α-helical loop of 20 amino acid residues (Asp^{484}–Gly^{504}) lies over the NADPH binding cleft. During oxidase activation, this loop is thought to move aside to allow NADPH to reach its binding site and deliver electrons to FAD. In this activated conformation, this loop is able to bind cytosolic factors. Yet we cannot speculate on the chronology of such events on the oxidase activation process. This result is also consistent with the assembly defect observed in an X^+CGD patient's neutrophils with a D500G missense mutation in Nox2 (30). However, it was reported that the deletion of Nox2 residues 488–497 did not affect translocation of $p47^{phox}$ and $p67^{phox}$ but only electron transfer from NADPH to FAD (40). Meanwhile, in this last case, deletion of the small region encompassing residues 488–497 conserves the acidic amino acids Asp^{484} and Asp^{500}, which seems to be essential to maintain the oxidase activity and the complex assembly. Asp^{500} of Nox2 is probably a crucial charged amino acid because whatever mutation was introduced, the oxidase activity and the $p47^{phox}$ translocation were inhibited.

To determine whether the inhibition of oxidase activity and/or the defect of complex assembly in mutant PLB-985 cells were associated with the electron transfer process from NADPH to FAD, we measured the INT reductase activity in purified plasma membranes from all the mutant transfected X-CGD PLB-985 cells (Fig. 8). This activity was abolished only in mutant PLB-985 cells of the α-helical loop ^{484}DESQANHFAVHHDEEKD^{500} of Nox2, whereas a $p47^{phox}$ translocation defect was also demonstrated. This suggests that the assembly of the NADPH oxidase complex is closely related to the electron transfer process from NADPH to FAD. Asp^{500} is possibly involved in the direct binding with cytosolic factors, resulting in the liberation of the NADPH binding site, as proposed by Taylor *et al.* (28). In addition, this C-terminal region of Nox2 is near the potential binding site for the adenine unit of NADPH (^{504}GLKQ^{507}). However, the electron transfer process can be dissociated from the assembly of the enzyme. Indeed in a study of an X^+CGD case, which was induced by a mutation that converted Gln^{507}-Lys^{508}-thr^{509} into His-Ile-Trp-Ala in a region near the potential binding site of NADPH, the translocation of both $p47^{phox}$ and $p67^{phox}$ to the membrane fractions of the patient's neutrophils was normal, indicating that this region is important for a correct electron transfer but not for the assembly of the oxidase complex (63). In addition, in the X^+CGD case resulting from a deletion of residues 488–497 in Nox2 reproduced in the X-CGD PLB-985 cells, cytosolic factor translocation occurred normally, whereas electron transfer from NADPH to FAD was defective (40). In the mutants of the D-loop (K195A/E, R198E, R199E, and RR198199QQ/AA), although the assembly of the oxidase complex and the electron transfer from NADPH to FAD were normal, the NADPH oxidase activity was totally abolished. The D-loop is localized close to the V transmembranous passage in the N-terminal part of Nox2, which has been proposed as being involved in heme binding. We speculate that this region might be involved in electron transfer from the FAD to the hemes. This hypothesis is currently under investigation in our laboratory.

Finally, we can conclude that charged amino acids of the D-loop (Lys^{195}, Arg^{198}, and Arg^{199}) and of the C-terminal region encompassing residues 484–500 (Asp^{484}, His^{490}, and Asp^{500}) are essential to maintain the NADPH oxidase activity in phagocytic cells. The D-loop of Nox1, -2, -3, and -4 is probably an important functional domain for the active conformational structure of Nox2, leading the electron transfer from FAD to oxygen, whereas the potential α-helical loop of the C-terminal tail of Nox2 is involved in the binding of cytosolic factors and in the electron transfer process from NADPH to FAD. The study of the relationship between these two events will allow us to better understand the molecular mechanisms of oxidase assembly.

Acknowledgments—We are grateful to Dr. Mary C. Dinauer for the generous gift of X-CGD PLB-985 cells. The 7D5 was kindly provided by Dr. Michio Nakamura. The antibodies 449 and 48 were generous gifts from Dr. D. Roos. We thank Pr. Philippe Gaudin for financial support and Michelle Guillot for technical assistance.

REFERENCES

1. Baldridge, C. W., and Gerard, R. W. (1933) *Am. J. Physiol.* **103,** 235–236
2. Cross, A. R., and Segal, A. W. (2004) *Biochim. Biophys. Acta* **1657,** 1–22
3. Sbarra, A. J., and Karnovsky, M. L. (1959) *J. Biol. Chem.* **234,** 1355–1362
4. Mandell, G. L. (1974) *Infect. Immun.* **9,** 337–341
5. Babior, B. M., Curnutte, J. T., and Kipnes, R. S. (1975) *J. Lab. Clin. Med.* **85,** 235–244
6. Babior, B. M., Kipnes, R. S., and Curnutte, J. T. (1973) *J. Clin. Invest.* **52,** 741–744
7. Dinauer, M. C. (1993) *Crit. Rev. Clin. Lab. Soc.* **30,** 329–369
8. Babior, B. M. (1999) *Blood* **93,** 1464–1476
9. Goldblatt, D., and Thrasher, A. J. (2000) *Clin. Exp. Immunol.* **122,** 1–9
10. Heyworth, P. G., Cross, A. R., and Curnutte, J. T. (2003) *Curr. Opin. Immunol.* **15,** 578–584
11. Reeves, E. P., Lu, H., Jacobs, H. L., Messina, C. G., Bolsover, S., Gabella, G., Potma, E. O., Warley, A., Roes, J., and Segal, A. W. (2002) *Nature* **416,** 291–297
12. Vignais, P. V. (2002) *Cell. Mol. Life. Sci.* **59,** 1428–1459
13. Segal, A. W., West, I., Wientjes, F., Nugent, J. H., Chavan, A. J., Haley, B., Garcia, R. C., Rosen, H., and Scrace, G. (1992) *Biochem. J.* **284,** 781–788
14. Rotrosen, D., Yeung, C. L., Leto, T. L., Malech, H. L., and Kwong, C. H. (1992)

Science **256,** 1459–1462
15. Cross, A. R., Rae, J., and Curnutte, J. T. (1995) *J. Biol. Chem.* **270,** 17075–17077
16. Yu, L., Quinn, M. T., Cross, A. R., and Dinauer, M. C. (1998) *Proc. Natl. Acad. Sci. U. S. A.* **95,** 7993–7998
17. Lapouge, K., Smith, S. J., Groemping, Y., and Rittinger, K. (2002) *J. Biol. Chem.* **277,** 10121–10128
18. Leto, T. L., Adams, A. G., and de Mendez, I. (1994) *Proc. Natl. Acad. Sci. U. S. A.* **91,** 10650–10654
19. DeLeo, F. R., Ulman, K. V., Davis, A. R., Jutila, K. L., and Quinn, M. T. (1996) *J. Biol. Chem.* **271,** 17013–17020
20. Sumimoto, H., Hata, K., Mizuki, K., Ito, T., Kage, Y., Sakaki, Y., Fukumaki, Y., Nakamura, M., and Takeshige, K. (1996) *J. Biol. Chem.* **271,** 22152–22158
21. DeLeo, F. R., and Quinn, M. T. (1996) *J. Leukoc. Biol.* **60,** 677–691
22. Ago, T., Kuribayashi, F., Hiroaki, H., Takeya, R., Ito, T., Kohda, D., and Sumimoto, H. (2003) *Proc. Natl. Acad. Sci. U. S. A.* **100,** 4474–4479
23. Paclet, M. H., Coleman, A. W., Vergnaud, S., and Morel, F. (2000) *Biochemistry* **39,** 9302–9310
24. Vergnaud, S., Paclet, M. H., El Benna, J., Pocidalo, M. A., and Morel, F. (2000) *Eur. J. Biochem.* **267,** 1059–1067
25. Dang, P. M., Cross, A. R., and Babior, B. M. (2001) *Proc. Natl. Acad. Sci. U. S. A.* **98,** 3001–3005
26. Dang, P. M., Cross, A. R., Quinn, M. T., and Babior, B. M. (2002) *Proc. Natl. Acad. Sci. U. S. A.* **99,** 4262–4265
27. Dusi, S., Nadalini, K. A., Donini, M., Zentilin, L., Wientjes, F. B., Roos, D., Giacca, M., and Rossi, F. (1998) *J. Immunol.* **161,** 4968–4974
28. Taylor, W. R., Jones, D. T., and Segal, A. W. (1993) *Protein Sci.* **2,** 1675–1685
29. Nakanishi, A., Imajoh-Ohmi, S., Fujinawa, T., Kikuchi, H., and Kanegasaki, S. (1992) *J. Biol. Chem.* **267,** 19072–19074
30. Leusen, J. H., de Boer, M., Bolscher, B. G., Hilarius, P. M., Weening, R. S., Ochs, H. D., Roos, D., and Verhoeven, A. J. (1994) *J. Clin. Invest.* **93,** 2120–2126
31. Thrasher, A. J., Keep, N. H., Wientjes, F., and Segal, A. W. (1994) *Biochim. Biophys. Acta* **1227,** 1–24
32. DeLeo, F. R., Yu, L., Burritt, J. B., Loetterle, L. R., Bond, C. W., Jesaitis, A. J., and Quinn, M. T. (1995) *Proc. Natl. Acad. Sci. U. S. A.* **92,** 7110–7114
33. Park, M. Y., Imajoh-Ohmi, S., Nunoi, H., and Kanegasaki, S. (1997) *Biochem. Biophys. Res. Commun.* **234,** 531–536
34. Zhen, L., Yu, L., and Dinauer, M. C. (1998) *J. Biol. Chem.* **273,** 6575–6581
35. Biberstine-Kinkade, K. J., Yu, L., and Dinauer, M. C. (1999) *J. Biol. Chem.* **274,** 10451–10457
36. Leusen, J. H., Meischl, C., Eppink, M. H., Hilarius, P. M., de Boer, M., Weening, R. S., Ahlin, A., Sanders, L., Goldblatt, D., Skopczynska, H., Bernatowska, E., Palmblad, J., Verhoeven, A. J., van Berkel, W. J., and Roos, D. (2000) *Blood* **95,** 666–673
37. Stasia, M. J., Lardy, B., Maturana, A., Rousseau, P., Martel, C., Bordigoni, P., Demaurex, N., and Morel, F. (2002) *Biochim. Biophys. Acta* **1586,** 316–330
38. Bionda, C., Li, X. J., Bruggen, R. V., Eppink, M., Roos, D., Morel, F., and Stasia, M. J. (2004) *Hum. Genet.* **115,** 418–427
39. Nauseef, W. M. (2004) *Histochem. Cell Biol.* **122,** 277–291
40. Yu, L., Cross, A. R., Zhen, L., and Dinauer, M. C. (1999) *Blood* **94,** 2497–2504
41. Lambeth, J. D. (2002) *Curr. Opin. Hematol.* **9,** 11–17
42. Bokoch, G. M., and Knaus, U. G. (2003) *Trends Biochem. Sci.* **28,** 502–508
43. Banfi, B., Clark, R. A., Steger, K., and Krause, K. H. (2003) *J. Biol. Chem.* **278,** 3510–3513
44. Geiszt, M., Lekstrom, K., Witta, J., and Leto, T. L. (2003) *J. Biol. Chem.* **278,** 20006–20012
45. Takeya, R., Ueno, N., Kami, K., Taura, M., Kohjima, M., Izaki, T., Nunoi, H., and Sumimoto, H. (2003) *J. Biol. Chem.* **278,** 25234–25246
46. Cheng, G., and Lambeth, J. D. (2004) *J. Biol. Chem.* **279,** 4737–4742
47. Tucker, K. A., Lilly, M. B., Heck, L., Jr., and Rado, T. A. (1987) *Blood* **70,** 372–378
48. Stasia, M. J., Brion, J. P., Boutonnat, J., and Morel, F. (2003) *J. Infect Dis.* **188,** 1593–1604
49. Verhoeven, A. J., Bolscher, G. J. M., Meerhof, L., van Zwieten, R., Keijer, J., Weening, R. S., and Roos, D. (1989) *Blood* **73,** 1686–1694
50. Batot, G., Paclet, M. H., Doussière, J., Vergnaud, S., Martel, C., Vignais, P. V., and Morel, F. (1998) *Biochim. Biophys. Acta* **406,** 188–202
51. Berthier, S., Paclet, M. H., Lerouge, S., Roux, F., Vergnaud, S., Coleman, A. W., and Morel, F. (2003) *J. Biol. Chem.* **278,** 25499–25508
52. Cohen-Tanugi, L., Morel, F., Pilloud-Dagher, M. C., Seigneurin, J. M., François, P., Bost, M., and Vignais, P. V. (1991) *Eur. J. Biochem.* **202,** 649–655
53. Cross, A. R., Yarchover, J. L., and Curnutte, J. T. (1994) *J. Biol. Chem.* **269,** 21448–21454
54. Bradford, M. M. (1976) *Anal. Biochem.* **72,** 248–254
55. Smith, P. K., Krohn, R. I., Hermanson, G. T., Mallia, A. K., Gartner, F. H., Provenzano, M. D., Fujimoto, E. K., Goeke, N. M., Olson, B. J., and Klenk, D. C. (1985) *Anal. Biochem.* **150,** 76–85
56. Zhen, L., King, A. A., Xiao, Y., Chanock, S. J., Orkin, S. H., and Dinauer, M. C. (1993) *Proc. Natl. Acad. Sci. U. S. A.* **90,** 9832–9836
57. Pedruzzi, E., Fay, M., Elbim, C., Gaudry, M., and Gougerot-Pocidalo, M. A. (2002) *Br. J. Haematol.* **117,** 719–726
58. Stasia, M. J., Bordigoni, P., Floret, D., Brion, J. P., Bost-Bru, C., Michel, G., Gatel, P., Durant-Vital, D., Voelckel, M. A., Li, X. J., Guillot, M., Maquet, E., Martel, C., and Morel, F. (2005) *Hum Genet.***116,** 72–82
59. Rae, J., Newburger, P. E., Dinauer, M. C., Noack, D., Hopkins, P. J., Kuruto, R., and Curnutte, J. T. (1998) *Am. J. Hum. Genet.* **62,** 1320–1331
60. Roesler, J., Heyden, S., Burdelski, M., Schafer, H., Kreth, H. W., Lehmann, R., Paul, D., Marzahn, J., Gahr, M., and Rosen-Wolff, A. (1999) *Exp. Hematol.* **27,** 505–511
61. Bellavite, P., Serra, M. C., Davoli, A., and Rossi, F. (1982) *Inflammation* **6,** 21–29
62. Segal, A. W. (1989) *J. Clin. Invest.* **83,** 1785–1793
63. Azuma, H., Oomi, H., Sasaki, K., Kawabata, I., Sakaino, T., Koyano, S., Suzutani, T., Nunoi, H., and Okuno, A. (1995) *Blood* **85,** 3274–3277